

COMMUNICATIONS

On Neglecting Chemical Exchange Effects When Correcting *in Vivo* ³¹P MRS Data for Partial Saturation¹Ronald Ouwerkerk² and Paul A. Bottomley

Division of MR Research, Department of Radiology, Johns Hopkins University, School of Medicine, Baltimore, Maryland 21287

Received January 7, 2000; revised July 13, 2000

Signal acquisition in most MRS experiments requires a correction for partial saturation that is commonly based on a single exponential model for T_1 that ignores effects of chemical exchange. We evaluated the errors in ³¹P MRS measurements introduced by this approximation in two-, three-, and four-site chemical exchange models under a range of flip-angles and pulse sequence repetition times (T_R) that provide near-optimum signal-to-noise ratio (SNR). In two-site exchange, such as the creatine-kinase reaction involving phosphocreatine (PCr) and γ -ATP in human skeletal and cardiac muscle, errors in saturation factors were determined for the progressive saturation method and the dual-angle method of measuring T_1 . The analysis shows that these errors are negligible for the progressive saturation method if the observed T_1 is derived from a three-parameter fit of the data. When T_1 is measured with the dual-angle method, errors in saturation factors are less than 5% for all conceivable values of the chemical exchange rate and flip-angles that deliver useful SNR per unit time over the range $T_1/5 \leq T_R \leq 2T_1$. Errors are also less than 5% for three- and four-site exchange when $T_R \geq T_1^*/2$, the so-called "intrinsic" T_1 's of the metabolites. The effect of changing metabolite concentrations and chemical exchange rates on observed T_1 's and saturation corrections was also examined with a three-site chemical exchange model involving ATP, PCr, and inorganic phosphate in skeletal muscle undergoing up to 95% PCr depletion. Although the observed T_1 's were dependent on metabolite concentrations, errors in saturation corrections for $T_R = 2$ s could be kept within 5% for all exchanging metabolites using a simple interpolation of two dual-angle T_1 measurements performed at the start and end of the experiment. Thus, the single-exponential model appears to be reasonably accurate for correcting ³¹P MRS data for partial saturation in the presence of chemical exchange. Even in systems where metabolite concentrations change, accurate saturation corrections are possible without much loss in SNR. © 2001

Academic Press

Key Words: chemical exchange; saturation factors; longitudinal relaxation; dual angle method; progressive saturation; creatine kinase; ³¹P MRS.

INTRODUCTION

To optimize the signal-to-noise ratio (SNR) per unit time, practical *in vivo* magnetic resonance spectroscopy (MRS) experiments must usually be performed with repetition times (T_R) that do not allow complete relaxation between repeat acquisitions (I). The signals must then be corrected for partial saturation if they are to be compared with signals acquired with different T_R values or if the spectra are to be used to interpret pathological changes or to determine absolute concentrations.

There are basically two methods of determining the partial saturation correction. The first is to record a fully relaxed signal for each experiment and measure a saturation factor. Unfortunately, this negates the efficiency of the short T_R experiment and is impractical for many *in vivo* MRS studies unless spatial localization is omitted for the long T_R experiment (2). The second method is to calculate a saturation correction using separately measured longitudinal relaxation times, T_1 , and an appropriate model for relaxation. This method is valid if the T_1 values do not vary between experiments (2) and if the experimental parameters and model used for calculating the saturation factors are valid. The standard model employed for correcting *in vivo* MRS measurements for saturation assumes monoexponential T_1 relaxation.

Recently, it has been suggested that ignoring the effects of chemical exchange by applying saturation corrections based on a single-exponential relaxation model to resonances that are undergoing chemical exchange would lead to large quantification errors (3–5). The nub of the argument is that chemical exchange renders the observed T_1 relaxation behavior multiexponential when the relaxation rates of the exchanging species differ. A corollary to this argument is that such multiexponential behavior will depend on factors that affect the chemical

¹ Supported by NIH Grants R01 HL56882-01, R01-HL61912-01, and R21 HL62332-01.

² To whom correspondence should be addressed at Department of Radiology, Johns Hopkins University, JHOC Room 4250, 601 N. Caroline Street, Baltimore, MD 21287-0845. Fax: (410) 614-1977. E-mail: rouwerke@mri.jhu.edu.

exchange components including the equilibrium magnetizations and the reaction rate constants, as well as the usual T_R and flip-angle parameters.

A specific *in vivo* example is the chemical exchange of high-energy (γ -) phosphate between adenosine triphosphate (ATP) and phosphocreatine (PCr), via the creatine-kinase (CK) reaction in muscle, as observed by phosphorus (^{31}P) MRS. A valid approach for eliminating potential errors in saturation corrections due to the effects of chemical exchange in the CK system is to accurately measure all of the exchange and relaxation rates for the system and to use them to calculate the saturation corrections based on mathematically correct solutions of the Bloch equations modified for systems with chemical exchange (3–6). Alternatively, one could again avoid the saturation correction altogether by performing fully relaxed experiments. However, both of these options are arguably impractical for *in vivo* localized ^{31}P MRS where the time required to acquire metabolite data from small volume elements (voxels) with sufficient SNR to measure both relaxation and exchange rates becomes prohibitive. In any case, this solution has thus far not been implemented for human studies and, moreover, all reported human ^{31}P CK metabolite T_1 's and saturation-corrected metabolite ratios and concentrations to date are based on a single-exponential characterization (7).

Clearly, these concerns raised about the accuracy of mono-exponential-based saturation corrections in the presence of chemical exchange (3–5) could undermine metabolite quantification in virtually all human and animal ^{31}P MRS studies performed under partially saturated conditions. However, other calculations using a three-site exchange model for the CK reaction in skeletal muscle suggest that the observed magnetization of each metabolite, the quantity that is relevant to the measurement of metabolite ratios and concentrations, may actually vary little with exchange rates in the range $0 \leq k \leq 20 \text{ [s}^{-1}\text{]}$ as a function of T_R for $1 \leq T_R \leq 8 \text{ [s]}$ in a simple 90° pulse-and-acquire experiment (6).

It is certainly more practical to approximate the relaxation behavior of exchanging species with a single-exponential model and to ignore the effects of chemical exchange. The observed T_1 's thus measured may well differ from the T_1 's of the same moieties if they could be measured in the absence of chemical exchange. However, the single exponential approximation would *not* be a problem for providing saturation corrections for the purpose of CK metabolite quantification if these observed T_1 's correctly predicted the fully relaxed magnetization.

Therefore, we analyzed the errors that would be introduced by ignoring the effects of chemical exchange in ^{31}P MRS studies of CK metabolism, as they are commonly performed in skeletal muscle and heart under practical conditions that optimize the SNR per unit time. Specifically, the magnitude of errors introduced in a conventional pulse-and-acquire experiment when best-fit monoexponential relaxation and relaxation corrections are assumed was determined by comparing the

saturation-corrected magnetizations to those calculated from the two-site exchange model (3, 4) over a broad range of T_R , T_1 , and k values. The errors in the dual-angle method used for measuring an assumed monoexponential T_1 of many human ^{31}P CK metabolites (7, 8) were also evaluated for the two-site model and for a three-site exchange model for human muscle using the matrix format of the exchange-modified Bloch equations (5, 6). Additional calculations were performed on a cyclic four-site exchange system to test whether errors in saturation corrections caused by neglecting chemical exchange worsen with increasing numbers of exchange sites.

Finally, changes in the equilibrium magnetization, or concentration, of any exchanging species can affect the apparent T_1 of the other exchanging species to some degree (5, 6). Therefore, as a relevant example, the effect of a net transfer of phosphate from PCr to Pi due to PCr depletion in exercising muscle was simulated using a three-site exchange model with PCr depletions of up to 95% of the initial concentration. In order to account for changes in the observed T_1 's as a function of the PCr concentration that the theory (3–6) predicts, a simple, practical interpolation method was tested: saturation corrections were based on T_1 's interpolated from observed T_1 's measured at the start and at the end of the PCr depletion experiment.

In general, these analyses show that the deviations from single-exponential behavior due to chemical exchange encountered in most steady-state one-pulse *in vivo* ^{31}P NMR experiments of CK metabolism appear to be very small except at very short T_R 's and relatively large flip-angles.

THEORY

The Single Exponential Model

In single-pulse MRS experiments, optimum SNR per unit time is achieved with flip-angles $\varphi \leq 90^\circ$ and $T_R \leq T_1$, the observed T_1 . The usual saturation factor for monoexponential longitudinal relaxation based on the Bloch equations in the absence of chemical exchange is

$$\text{SF}(\varphi, T_R, T_1) = \frac{S(\varphi, T_R, T_1)}{M_0} = \frac{\sin(\varphi) \cdot (1 - \exp(-T_R/T_1))}{(1 - \exp(-T_R/T_1) \cdot \cos(\varphi))}, \quad [1]$$

where $S(\varphi, T_R, T_1)$ is the partially saturated signal and M_0 is the equilibrium magnetization (2).

The Two-Site Exchange Model

Spencer and colleagues (3, 4) derived equations for the saturation factors, SFX^A and SFX^B , for two exchanging species, A and B, in steady-state equilibrium from the Bloch–McConnell equations (9):

$$\text{SFX}^A(T_R, \varphi) = \sin \varphi \left(1 + q_1 \frac{(1 - \cos \varphi) \exp(D_+ T_R)}{(1 - \cos \varphi \exp(D_+ T_R))} + q_2 \frac{(1 - \cos \varphi) \exp(D_- T_R)}{(1 - \cos \varphi \exp(D_- T_R))} \right) \quad [2]$$

$$\text{SFX}^B(T_R, \varphi) = \sin \varphi \left(1 + r_1 \frac{(1 - \cos \varphi) \exp(D_+ T_R)}{(1 - \cos \varphi \exp(D_+ T_R))} + r_2 \frac{(1 - \cos \varphi) \exp(D_- T_R)}{(1 - \cos \varphi \exp(D_- T_R))} \right), \quad [3]$$

with

$$D^+(T_1^{*A}, T_1^{*B}, k_{AB}) = 0.5[-(1/T_1^{*A} + 1/T_1^{*B} + k_{AB} + k_{BA}) + \text{disc}] \quad [4]$$

$$D^- = D^+ - \text{disc}, \quad [5]$$

$$\text{disc} = \sqrt{[(1/T_1^{*A} - 1/T_1^{*B} + k_{AB} - k_{BA})^2 + 4 \cdot k_{AB} \cdot k_{BA}]}, \quad [6]$$

$$q_1 = 0.5[(1/T_1^{*A} - 1/T_1^{*B} - k_{AB} - k_{BA})/\text{disc} - 1], \quad [7]$$

$$q_2 = -1 - q_1, \quad [8]$$

$$r_1 = 0.5[(1/T_1^{*B} - 1/T_1^{*A} - k_{AB} - k_{BA})/\text{disc} - 1], \quad [9]$$

and

$$r_2 = -1 - r_1. \quad [10]$$

The constants q_1 , q_2 , r_1 , and r_2 and the exponential coefficients D^+ and D^- are all functions of the so-called ‘‘intrinsic’’ T_1 ’s of the exchanging species, T_1^{*A} and T_1^{*B} , that would be observed if there were no exchange, and the forward and reverse chemical exchange rate constants, k_{AB} and k_{BA} . Note that k_{AB} and k_{BA} are not independent variables since $k_{BA} = k_{AB} M_{0A}/M_{0B}$.

It is the differences between Eqs. [2]–[3] and [1], and particularly the appearance of the third term in Eqs. [2] and [3], that has the potential to cause errors in quantification when Eq. [1] is assumed in cases where chemical exchange is present (3, 4). However, because the exponential coefficients D^+ and D^- are both negative and $D^+ > D^-$, the third term approaches zero faster than the other terms as T_R increases. If this term approaches zero and coefficients q_i or r_i are close to unity, Eqs. [2] and [3] reduce to Eq. [1]. Consequently, there exist combinations of relaxation and chemical exchange rates such that Eqs. [2] and [3] can effectively be approximated by the single-exponential model. We shall examine the conditions under which this occurs as a function of the forward rate constant over the range of T_R values and flip-angles that provide optimum SNR per unit time.

The n -Site Exchange Model

The solutions of the Bloch–McConnell equations (9) in the presence of chemical exchange between more than two sites are more complex and are best treated in the matrix form (5, 6)

$$\frac{d\mathbf{M}}{dt} = \mathbf{A}\mathbf{M} + \mathbf{C}, \quad [11]$$

where $\mathbf{M} = (M_{S_1}, M_{S_2}, \dots, M_{S_n})$ is a magnetization vector composed of the n magnetizations from each of the i exchanging species, S_i , \mathbf{A} is a matrix with elements

$$A_{ij} = \left\{ \frac{1}{T_1^{*S_i}} + \sum_{j \neq i} k_{S_i S_j} \right\}, \text{ for } i = j; \quad \text{and}$$

$$A_{ij} = k_{S_j S_i} \text{ for } i \neq j \quad [12]$$

$$\mathbf{C} = \left(\frac{M_{0S_1}}{T_1^{*S_1}}, \frac{M_{0S_2}}{T_1^{*S_2}}, \dots, \frac{M_{0S_n}}{T_1^{*S_n}} \right), \quad [13]$$

and $T_1^{*S_i}$ is the ‘‘intrinsic’’ T_1 of S_i , and the $k_{S_j S_i}$ is the exchange rate from S_j to S_i . The solution of Eq. [11] for the steady-state magnetization at T_R is then calculated from

$$M_{ss}(T_R, \varphi) = (\mathbf{I} - \cos \varphi \cdot e^{A T_R})^{-1} (e^{A T_R} - \mathbf{I}) \cdot \mathbf{A}^{-1} \cdot \mathbf{C}, \quad [14]$$

as in Eq. [26] of the paper by Spencer and Fishbein (5), where \mathbf{I} is the identity matrix, which reduces to Eq. [4] of the paper by Binzoni and Cerretelli (6) at 90° flip angles.

METHODS

Our analysis focuses on two tissue types studied frequently *in vivo* by ^{31}P MRS where the chemical exchange of PCr and γ -ATP via CK metabolism may affect saturation corrections and consequently quantification. For the first tissue, skeletal muscle, parameters were taken from Horska and Spencer as listed in Table 1 (4). For the second tissue, heart muscle, we chose a PCr:ATP concentration ratio of 1.5:1. The intrinsic T_1 ’s for PCr and γ -ATP in human heart are not well determined. We shall assume that the molecular-level environment for PCr and γ -ATP is comparable to that observed in skeletal muscle so that the intrinsic T_1 ’s differ by a factor of three: $T_1^{*A} = 6$ s and $T_1^{*B} = 2$ s. The shorter observed T_1 ’s of human myocardial PCr and γ -ATP reported in the literature (7) differ from these values, perhaps due to the effects of chemical exchange.

In choosing the range of conditions that provide optimum SNR per unit time for the present analysis, we note that while the optimum flip-angle, the Ernst angle, occurs when $\cos(\varphi) =$

TABLE 1
Parameters Used for Calculations of Saturation Factors and Simulations of T_1 Measurements with the Two-Site Model

Simulation parameters	Skeletal muscle	Heart muscle
[PCr]:[ATP]:[Pi]	4.6:1	1.5:1
T_1^{*A} , PCr	6.7	6
T_1^{*B} , γ -ATP	2.3	2
$k_{A \rightarrow B}$	0.27	0.25
T_1 PCr literature (7)	6.52	4.37
T_1 γ -ATP literature (7)	4.32	2.52

$\exp(-T_R/T_1)$ (I), in practice most *in vivo* experiments are designed to measure several metabolites. Thus, either the SNR must be optimized for the most important metabolite, or a compromise must be chosen to yield near-optimum SNR for all metabolites of interest. Large flip-angles have broader ranges of T_R values that yield $\geq 95\%$ of the best SNR than small flip-angles and therefore offer the best opportunity for optimizing SNR per unit time for multiple metabolites exhibiting different T_1 's. For $\varphi = 90^\circ$, the optimum SNR per unit time occurs at $T_R = 1.256 T_1$, but the SNR is reduced by only 5% over the broad range $0.77 T_1 \leq T_R \leq 2.09 T_1$. To optimize the SNR for two exchanging metabolites, the optimum repetition time, T_{RO} , was calculated from the geometric mean of the (observed, not intrinsic) T_1 values, $T_{RO} = 1.256 \sqrt{(T_1^A \cdot T_1^B)}$ (7).

Numerical analysis was performed with Matlab (Mathworks, Natick, MA) running on a Sparc 10 workstation (Sun Microsystems, Palo Alto, CA) and with Excel (Microsoft, Seattle, WA) running on an Apple G4 (Apple, Cupertino, CA).

Analysis of the Two-Site Exchange Model

To analyze the importance of the third term in Eqs. [2] and [3] for the two-site exchange model, its magnitude was determined as a function of k_{AB} , T_R , and φ , with T_R varied from 0 to 30 s with $\varphi = 90^\circ$ and at $T_R = 1$ s for flip-angle $\varphi = 0-90^\circ$. The forward rate constant, k_{AB} , was varied between 0 and 1.5 [s^{-1}]. Because the part of Eqs. [2] and [3] between the outer brackets is normalized, the magnitude of the third term (the second exponential term) is a good indicator for the maximum relative error that can be introduced in the saturation factor by ignoring this term.

The progressive saturation measurement was simulated with a 90° flip-angle and a T_R that varied from 0 to 30 s for T_1 's and forward rate constants as listed in Table 1. Six measurement points were chosen, at $T_R = 0.25, 0.5, 1, 2T_{RO}$, and $4T_{RO}$, with T_{RO} calculated assuming the literature T_1 's listed in Table 1, and a sixth point at $T_R = 5T_1^A$. Saturation factors were calculated from Eqs. [2] and [3] for these T_R values, then an observed T_1 , T_1^{obs} , was determined from a three-parameter nonlinear least-squares fit to the normalized signal (10):

$$SF = P \cdot [1 - Q \cdot \exp(-T_R/T_1^{obs})], \quad [15]$$

with P and Q constants. Using this fitted T_1^{obs} and Q , predicted saturation factors were calculated and these were compared to saturation factors determined directly from Eqs. [2] and [3].

With the dual-angle method of measuring T_1 , T_1^{obs} is determined from the ratio R of partially saturated signals acquired at flip-angles of $\alpha = 15^\circ$ and $\beta = 60^\circ$ assuming monoexponential relaxation (8). These flip-angles were chosen to provide the best SNR and sensitivity to T_1 . To evaluate the effects of chemical exchange on observed T_1 's measured by this method, the observed T_1 at a given T_R was calculated from the standard monoexponential based formula (8),

$$T_1 = -T_R / \ln \left(\frac{\sin \alpha - R \sin \beta}{\cos \beta \sin \alpha - R \cos \alpha \sin \beta} \right), \quad [16]$$

with $R = M_{ss}(\alpha)/M_{ss}(\beta) = SFX(\alpha)/SFX(\beta)$, the ratio of the partially saturated signals, which is equivalent to the ratio of the saturation factors. From this T_1^{obs} , the saturation factors for species A and B predicted by Eq. [1], $SF(\varphi, T_R, T_1^{obs})$, were calculated as a function of flip-angle, φ , in the range $15^\circ \leq \varphi \leq 60^\circ$ for the same T_R . The fractional error in the saturation factors predicted by the monoexponential model and that predicted with the effects of chemical exchange included were then calculated for heart and skeletal muscle as

$$\text{error}(T_R, \varphi) = (SF - SFX)/SFX. \quad [17]$$

Three- and Four-Site Exchange Models

The T_1 's and equilibrium magnetizations used for the calculations on three- and four-site exchange models based on Eqs. [11]–[14] are given in Table 2, which again uses the data of Horská and Spencer (4) plus an estimate of T_1^{*Pi} based on a

TABLE 2
Parameters Used for Calculations of Saturation Factors and Simulations of T_1 Measurements with Three- and Four-Site Exchange Models

Skeletal muscle, three-site linear exchange				
Species	PCr	ATP	Pi	
T_1^* [s]	6.7	2.3	5.5	
Concentration [mM]	28	4.5	2	
Four site cyclic exchange				
Species	A	B	C	D
T_1^* [s]	5	3	1	0.5
M_0 [arb. units]	1	1	1	1

literature mean of 5.3 s (7). The k values used to simulate a three-site exchange in skeletal muscle are, in matrix form,

$$\mathbf{K}_{\text{muscle}} = \begin{pmatrix} 0 & k_{\text{ATP,PCr}} & 0 \\ k_{\text{PCr,ATP}} & 0 & k_{\text{Pi,ATP}} \\ 0 & k_{\text{ATP,Pi}} & 0 \end{pmatrix} = \begin{pmatrix} 0 & 1.68 & 0 \\ 0.27 & 0 & 1.125 \\ 0 & 0.5 & 0 \end{pmatrix}. \quad [18]$$

Four-site exchange was explored with a normalized expansion of the cyclic three-site model presented by Spencer and Fishbein (5):

$$\mathbf{K}_{\text{cyc}} = \begin{pmatrix} 0 & k_{\text{BA}} & 0 & k_{\text{DA}} \\ k_{\text{AB}} & 0 & k_{\text{CB}} & 0 \\ 0 & k_{\text{BC}} & 0 & k_{\text{DC}} \\ k_{\text{AD}} & 0 & k_{\text{CD}} & 0 \end{pmatrix} = \begin{pmatrix} 0 & 1 & 0 & 1 \\ 1 & 0 & 1 & 0 \\ 0 & 1 & 0 & 1 \\ 1 & 0 & 1 & 0 \end{pmatrix}. \quad [19]$$

With these data the observed steady-state magnetization, $M_{\text{ss}}(T_{\text{R}}, \varphi)$, was calculated for each species at flip-angles of 15, 60, and 35° over the range $0.5 \leq T_{\text{R}} \leq 5$ s. The values of M_{ss} at 15 and 60° flip angles were used to calculate the T_1 's and saturation factors, $\text{SF}(T_{\text{R}}, 35^\circ)$, using Eqs. [16] and [1], respectively. The relative error in the observed equilibrium magnetization as a function of the observation flip-angle and T_{R} due to the neglect of exchange effects is

$$\text{error}(T_{\text{R}}, \varphi) = \left| \frac{M_{\text{ss}}(T_{\text{R}}, \varphi)}{\text{SF}(T_{\text{R}}, \varphi)} - M_0 \right| / M_0, \quad [20]$$

where M_0 is the true equilibrium magnetization given in Table 2.

Skeletal Muscle with PCr Depletion

The effect of varying metabolite concentrations on saturation corrections and monoexponential dual-angle T_1 measurements was evaluated in the three-site linear exchange model for skeletal muscle at T_{R} 's of 1 and 2 s by iterating Eq. [14] with varying PCr and Pi concentrations. The initial PCr and Pi concentrations were 28 and 2 [mM], respectively. They were varied in steps of 1% to 1.4 [mM] for PCr and 28.6 [mM] for Pi, in order to simulate a net transfer of PCr to Pi, as would occur, for example, with PCr depletion in a muscle exercise study. The initial matrix \mathbf{A} for Eq. [12] was calculated with $\mathbf{K}_{\text{muscle}}$ as given in Eq. [18] and T_1^* values from Table 2. At each change in concentrations the reverse flux terms ($k_{\text{ATP,PCr}}$ and $k_{\text{Pi,ATP}}$) in matrix \mathbf{A} were recalculated to maintain the chemical equilibrium conditions:

$$k_{\text{ATP,PCr}} \cdot [\text{ATP}] = k_{\text{PCr,ATP}} \cdot [\text{PCr}] \quad [21]$$

$$k_{\text{Pi,ATP}} \cdot [\text{Pi}] = k_{\text{ATP,Pi}} \cdot [\text{ATP}]. \quad [22]$$

T_{R} values of 1 and 2 s were chosen with flip-angles of 35 and 48°, respectively. These flip-angles are approximately equal to the Ernst angles calculated from the geometric mean of the observed T_1 's of PCr, ATP, and Pi that would result from a dual-angle measurement of the simulated three-site exchange data with these T_{R} values and the intrinsic T_1 values listed in Table 2. These flip-angles are also within $\pm 2^\circ$ of the Ernst angle calculated from the geometric mean of the observed *in vivo* T_1 's of PCr, ATP, and Pi reported in the literature (7). For the simulation, observed T_1 's were calculated for each PCr depletion step with Eq. [16] from $M_{\text{ss}}(T_{\text{R}}, \varphi = 15^\circ)$ and $M_{\text{ss}}(T_{\text{R}}, \varphi = 60^\circ)$. However, in a practical experiment it is not normally possible to continuously measure T_1 . Therefore, for the purpose of calculating saturation factors, T_1 values were linearly interpolated for each PCr level, based on values at the start and at the end of the PCr depletion experiment. Saturation factors were then derived from these interpolated T_1 's using Eq. [1]. Errors in the equilibrium magnetization were calculated from Eq. [20] using these (interpolated) saturation factors and values of $M_{\text{ss}}(T_{\text{R}} = 1, \varphi = 35^\circ)$ and $M_{\text{ss}}(T_{\text{R}} = 2, \varphi = 48^\circ)$ derived from Eq. [14].

The calculated $M_{\text{ss}}(T_{\text{R}}, \varphi)$ were also used to examine the cost in SNR of replacing acquisitions with near optimal flip-angles with dual-angle T_1 measurements. If the SNR cost were low, spectra obtained with the dual-angle method could be used as time points in a dynamic NMR experiment if the changes in metabolite concentrations are negligible over the time course of the T_1 experiment. The cost of the added T_1 measurements is the extra scan time needed to obtain adequate SNR with nonoptimal 15 and 60° flip-angles.

RESULTS

Analysis of the Two-Site Exchange Model

The calculations for skeletal muscle show that for exchanging species A, PCr, the third term in Eq. [2] never exceeds 0.01 (1%) over the entire range of T_{R} 's that yield 95% of the maximum SNR efficiency, as shown in Fig. 1A. For species B, γ -ATP, the third term of Eq. [3] exceeds 0.01 (1%) only in the regime of low T_{R} and low k_{AB} (Fig. 1B). In heart muscle, the magnitude of the third term is shown as a function of φ at $T_{\text{R}} = 1$ s in Figs. 1C and 1D. For $\varphi \leq 15^\circ$ the contribution from the third term is below 0.01 (1%) for all exchange rates for species A and for exchange rates $k_{\text{AB}} \geq 0.18$ [s⁻¹] for species B. At $\varphi = 60^\circ$, the contribution of the third term is higher, exceeding 0.01 (1%) for $k_{\text{AB}} \leq 0.45$ [s⁻¹] for species A (Fig. 1C) and $k_{\text{AB}} \leq 0.6$ [s⁻¹] for species B (Fig. 1D).

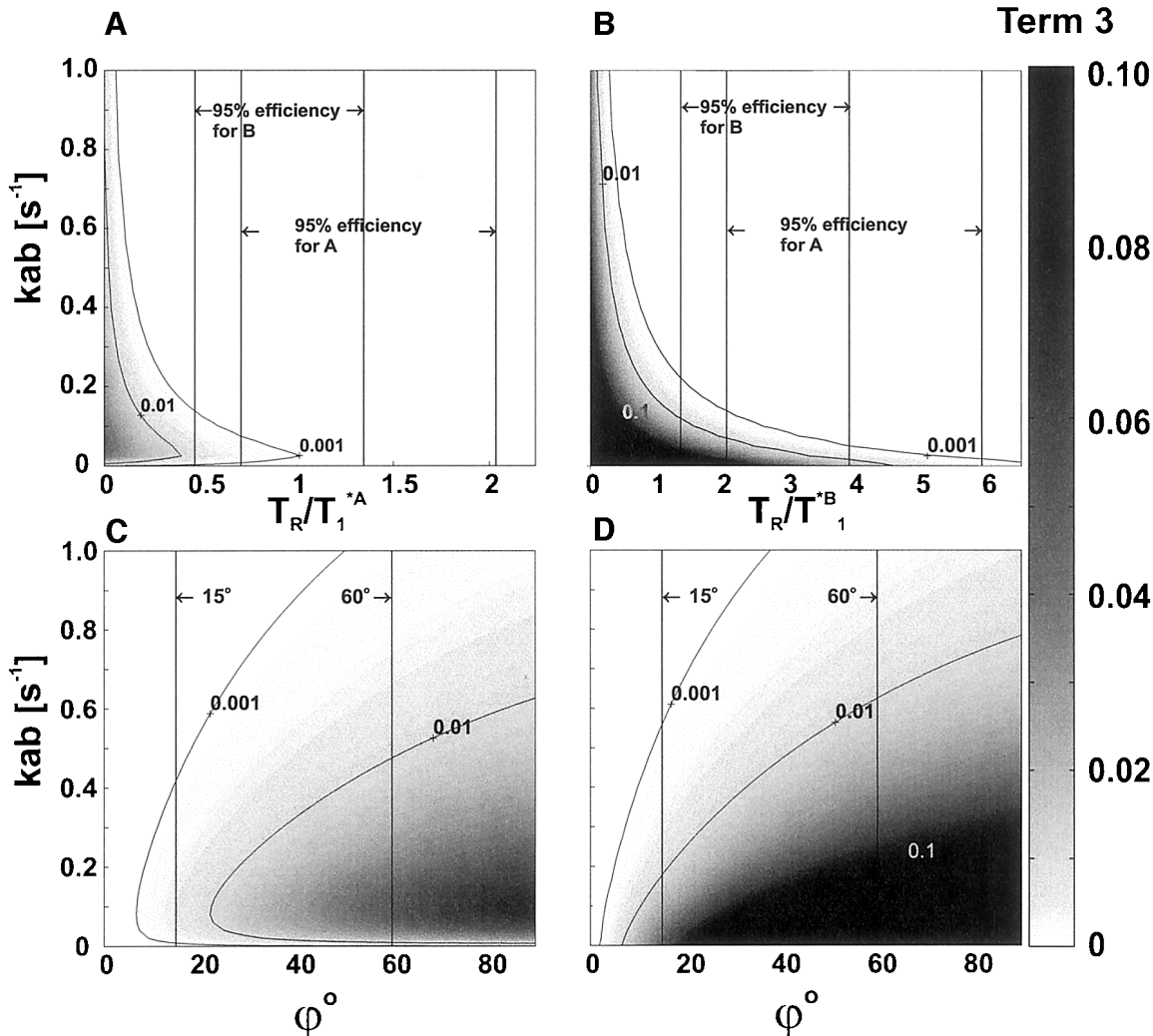


FIG. 1. (A) Contour plots (at 0.1, 0.01, 0.001) of the relative amplitude of the third terms of Eqs. [2] and [3] describing partial saturation in the presence of two-site chemical exchange plotted for skeletal muscle as a function of T_R with $\phi = 90^\circ$ for species A (A) and B (B). The relative amplitudes of the third terms of Eqs. [2] and [3] for heart muscle are plotted for species A and B in (C) and (D), respectively, as a function of flip-angle with $T_R = 1$ s. The parameters used for the calculations are given in Table 1. The boundaries for 95% efficiency in SNR per unit time were calculated from the literature T_1 's given in Table 1.

How these contributions translate into errors in the predicted saturation factors was evaluated with simulated T_1 measurements, as depicted in Fig. 2 for skeletal muscle. The variable T_R , progressive saturation experiment was simulated by fitting saturation factors calculated with Eqs. [2] and [3] to a single-exponential model with a three-parameter fit (Eq. [15]) assuming a value of $k_{AB} = 0.27$ [s⁻¹]. This value was derived from 10 normal human legs measured *in vivo* at rest by two different methods (11). The saturation factors calculated with the fitted parameters are indistinguishable from the original data points that were calculated from the two-site exchange model represented by Eqs. [2] and [3] (Fig. 2). Similar results were obtained for the heart, assuming a value of $k_{AB} = 0.25$ [s⁻¹]. In both tissues, the only noticeable deviation between the satura-

tion factors calculated with Eqs. [2], [3], and the predicted saturation factors obtained from the single-exponential fitted model occurs at very short T_R values. Here, the original data points pass through the origin while the three-parameter fit results in a small offset, which normally helps compensate for flip-angle errors in conventional T_1 studies (10). The magnitude of the errors in the saturation factors from the single-exponential fit is otherwise negligible.

The results of the calculations for the dual-angle T_1 method using Eqs. [2], [3], and [1] and [16] are shown for heart muscle, at $T_R = 1$ s in Fig. 3. The saturation factors predicted with the single-exponential model, Eq. [1], using an observed T_1 calculated with Eq. [16], are hardly distinguishable from the saturation factors calculated with Eqs. [2] and [3].

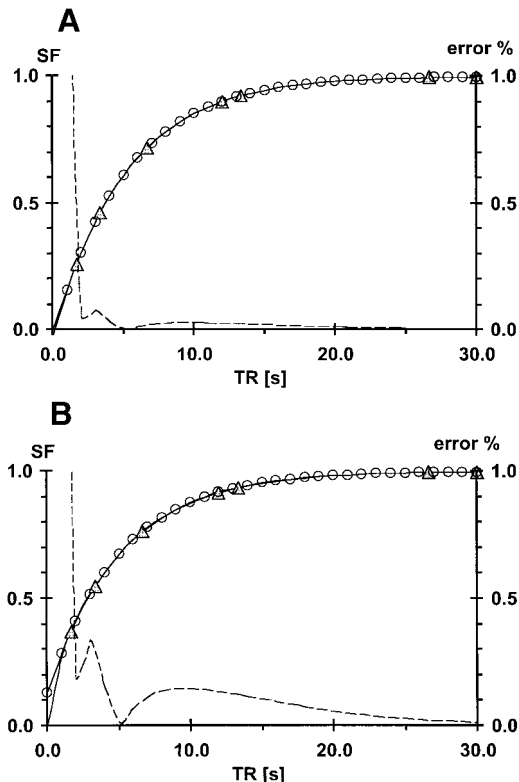


FIG. 2. Simulation of a progressive saturation T_1 measurement for skeletal muscle with two-site exchange parameters as in Table 1, except with $k_{AB} = 0.27 \text{ [s}^{-1}\text{]}$. The saturation factors calculated with Eq. [2] for species A (A), and Eq. [3] for species B (B), are shown as solid lines. The triangles indicate points selected for a three-parameter fit to the single-exponential Eq. [15]. Predicted saturation factors using the fitted parameters T_1^{obs} and Q are shown as open circles. The magnitude of the errors in the saturation factors as calculated with Eq. [17] is shown as a dashed line with values in percentages on the right-hand axis.

The maximum error in the saturation factors predicted by the dual-angle method for any excitation flip-angle in the range $15^\circ \leq \varphi \leq 60^\circ$ is shown in Fig. 4 for both tissues. For skeletal muscle, the errors in species A at $T_R = 1 \text{ s}$ are less than 3% for all k_{AB} (Fig. 4A). The errors are higher for species B, but these again decrease to about 3% or less if T_R is increased to 2 s (Fig. 4B). For cardiac muscle, the errors at $T_R = 1 \text{ s}$ are less than 4.5% for all values of k_{AB} , as shown in Fig. 4C. At $T_R = 2 \text{ s}$, the errors drop to 1.5% or less for all values of k_{AB} (Fig. 4D). All errors decrease further as the exchange rate increases above about $0.2 \text{ [s}^{-1}\text{]}$.

Analysis of the Three- and Four-Site Exchange Models

The relative errors in the equilibrium magnetization calculated assuming single-exponential T_1 measurements obtained by the dual-angle method decrease with increasing T_R , as shown in Fig. 5. In the range $T_R \geq 1 \text{ s}$, the errors are 4% or less

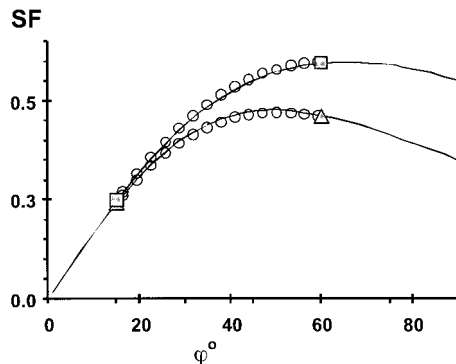


FIG. 3. Simulation of a dual-angle T_1 measurement for species A (slower relaxing species, bottom line) and B (the faster relaxing species, top line) assuming the two-site exchange parameters for heart muscle listed in Table 1 and a T_R of 1 s. The saturation factors (SFX) calculated with Eqs. [2] and [3] are shown as a solid line. The triangles and squares indicate the values of SFX calculated for 15° and 60° flip-angles that are used to compute observed T_1 's from Eq. [16] (triangles for species A, squares for species B). These observed T_1 's were used in the single-exponential model, Eq. [1], to calculate predicted saturation factors, represented by open circles.

for both the three- and the four-site exchange models. From Table 2, this corresponds to an intrinsic $T_1^*/2 < T_R$ for all metabolites.

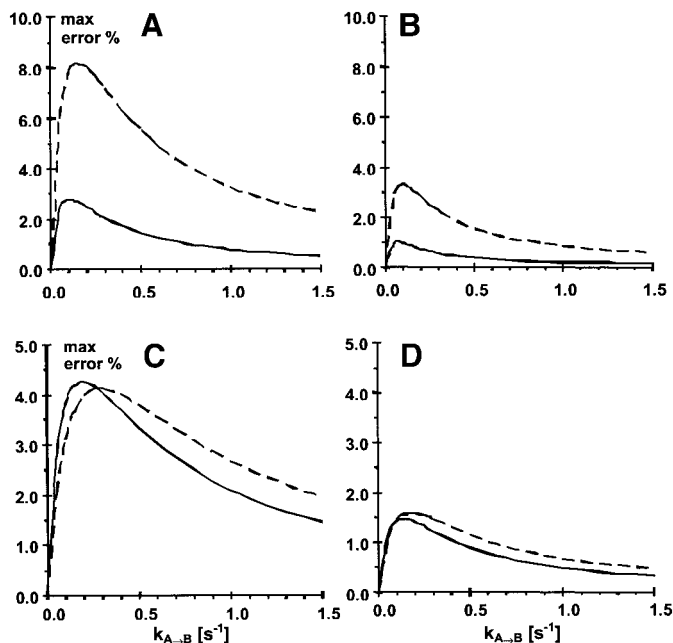


FIG. 4. The maximum error in saturation factor that can occur for any excitation flip-angle in the range $15^\circ \leq \varphi \leq 60^\circ$, as a function of the forward rate constant $k_{A..B}$ for skeletal (A, B) and heart (C, D) muscle, for the two-site exchange model. Solid and dashed curves correspond to species A and B, respectively. Errors are calculated at $T_R = 1 \text{ s}$ (A, C) and 2 s (B, D) with parameters as listed in Table 1.

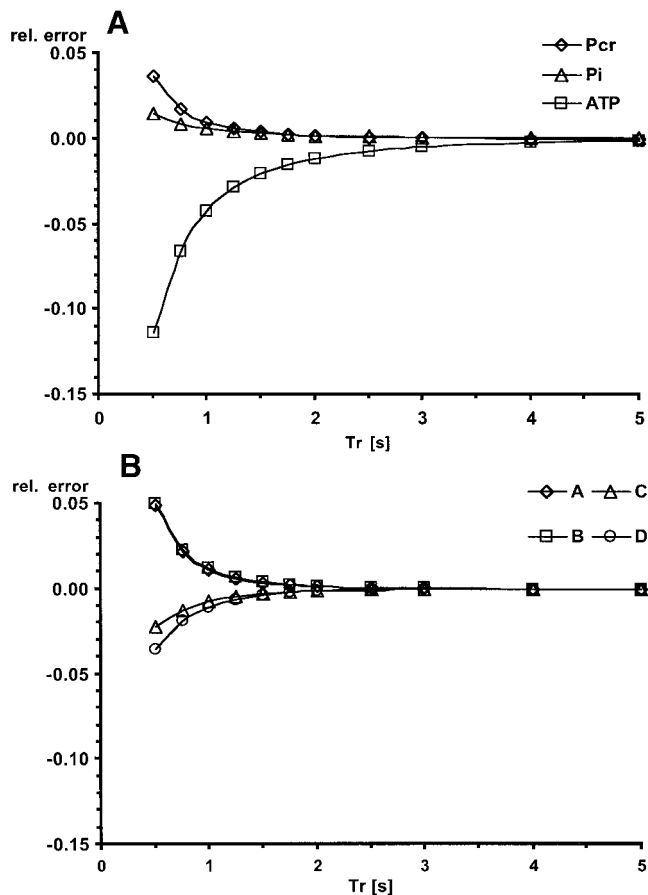


FIG. 5. The relative errors in saturation factors calculated for 35° excitation flip-angle as a function of T_R with n -site exchange rate constants given by Eqs. [18] and [19] and other parameters as listed in Table 2. The open symbols are the relative errors for each species in calculated M_0 when a dual angle T_1 measurement with flip-angles of 15 and 60° is used to correct the saturation for a measurement at 35° flip-angle. The solid lines are an interpolation of the points. (A) Skeletal muscle three-site linear exchange model. The errors for PCr are shown as open diamonds, for ATP as open squares, and for Pi as open triangles. (B) Four-site cyclic exchange model (species A, open diamonds; species B, open squares; species C, open triangles; species D, open circles).

Skeletal Muscle with PCr Depletion

In Figs. 6A and 6B, the input and estimated equilibrium magnetizations are shown for the three exchanging species, PCr, ATP, and Pi, in skeletal muscle for $T_R = 1$ –2 s. The linear interpolations of the observed T_1 's are reasonable approximations to the continuous observed T_1 's as a function of metabolite concentrations, as shown in Figs. 6C and 6D. The largest deviations between continuous and interpolated T_1 occur for Pi where the relative changes in concentrations are extremely large. Regardless, the estimated equilibrium magnetizations, as calculated with the saturation correction factors of Eq. [1], are surprisingly close to the equilibrium magnetizations used as input for the linear three-site exchange model, as shown by the plotted points in Figs. 6A and 6B. In fact, the errors in the

calculated equilibrium magnetizations are about 8% or less, being highest for ATP and half that or less for the other metabolites, as depicted in Figs. 6E and 6F, over the entire range of PCr depletion. Note that the errors for PCr and ATP are half again at the longer T_R of 2 s.

A disadvantage of using the longer T_R is that the SNR penalty for inserting the extra dual-angle T_1 measurements is slightly higher. A dual-angle T_1 measurement that yields the same SNR as two 48° acquisitions at $T_R = 2$ s takes about 2.2 times longer, whereas a dual-angle T_1 measurement that yields the same SNR as two 35° acquisitions at $T_R = 1$ s takes only a factor of 1.7 longer.

DISCUSSION

The analysis presented here shows that the errors introduced by approximating the multiple exponential relaxation model that results from inclusion of chemical exchange with a single-exponential function are limited by the experimental and intrinsic values of T_R , T_1 , k_{AB} , and φ . The need to maximize SNR per unit time in both acquisition of the T_1 information from which the saturation factors are derived and acquisition of *in vivo* spectral information places practical limitations on experimental parameters. It was found that, within these constraints as applied to practical human ^{31}P MRS protocols for studying CK metabolism in skeletal and heart muscle, the effects of two-site chemical exchange on corrections for partial saturation, using T_1 measurements based on a monoexponential model, are essentially negligible.

The largest exchange effects for the two-site model occur for the species B nuclei, γ -ATP in the cases studied, where there are conceivable combinations of T_R , T_1 , and k_{AB} that could introduce errors as large as 8%, compared with 3% for species A, PCr (Fig. 4). However, this can be avoided for the purpose of quantifying [ATP] or PCr/ATP ratios, by using the β -ATP resonance instead of γ -ATP (12), as has long been practiced by some groups (13). Larger errors might be generated if the observed T_1 's are used to generate saturation factors for extreme flip-angles or T_R values that deviate far from those at which the T_1 was measured (4, 5). In addition, large errors can result at short T_R values if T_1 data are fitted to monoexponential relaxation models using imprudent fitting procedures, including, for example, two-point fits or the forcing of fits to pass through the origin as one effectively does when predicting saturation factors from only two observations (4, 5).

One proposed strategy to minimize the errors in saturation corrections due to neglecting the effects of chemical exchange is to both perform the actual measurements and determine T_1 at very short T_R 's and large flip-angles (5). Although this approach yields observed T_1 's that are much closer to the so-called intrinsic T_1 's, Fig. 5 shows that the accuracy with which these T_1 's can predict the equilibrium magnetization is actually worse than the accuracy obtainable at longer T_R 's. Spencer and

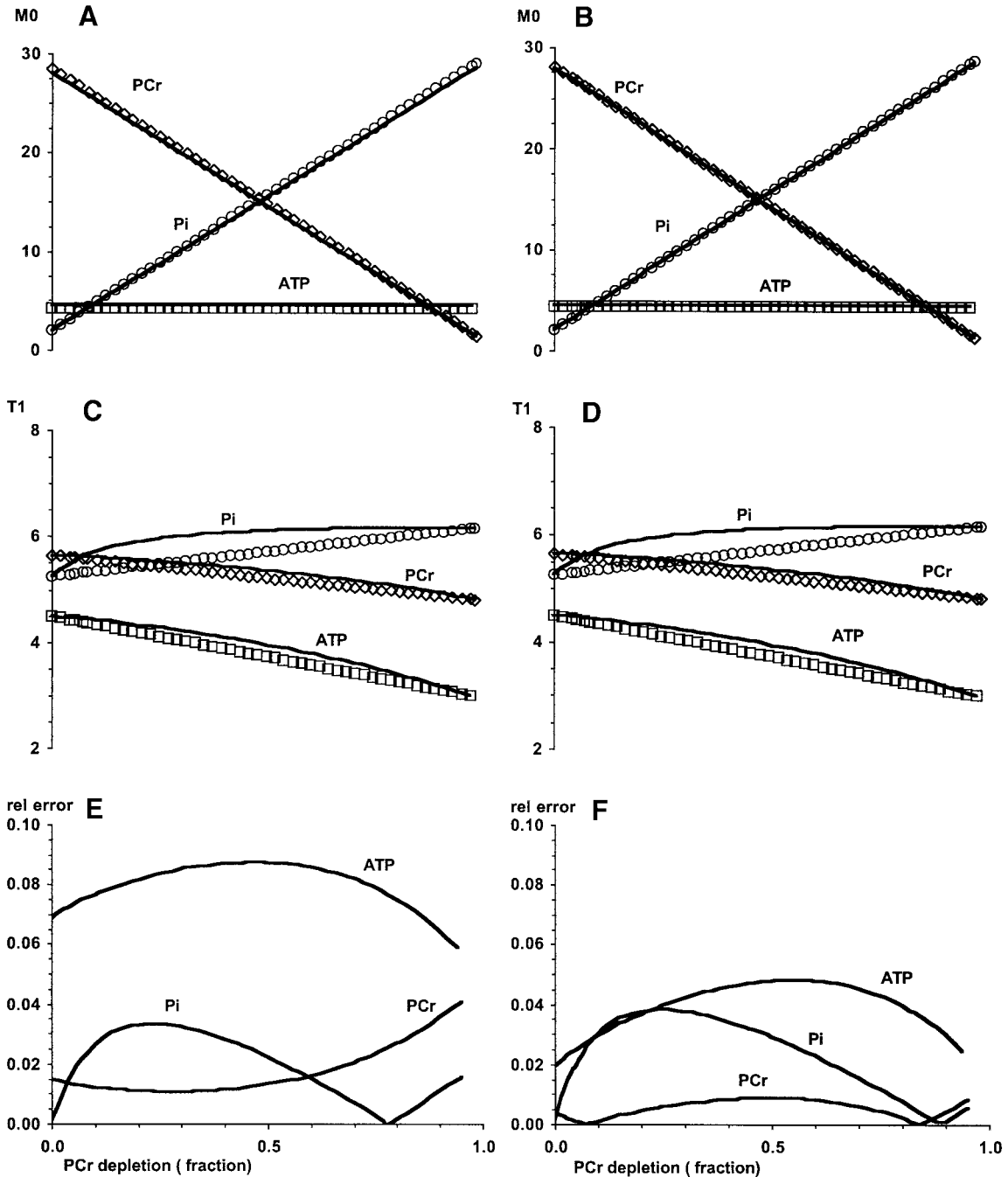


FIG. 6. The effect of PCr depletion on calculated equilibrium magnetizations in a linear three-site chemical exchange model of skeletal muscle for steady state acquisitions at $T_R = 1$ s and 35° flip-angle (A) and $T_R = 2$ s and 48° flip-angle (B), shown as open circles for Pi, open diamonds for PCr, and open squares for ATP. The true equilibrium magnetizations that were used as input for the model are shown as solid lines. The changes in the observed T_1 as a function of the fractional depletion of PCr are shown for $T_R = 2$ s in (C) and $T_R = 2$ s in (D) as solid lines. The interpolated T_1 values used for saturation corrections are shown as open circles for Pi, open diamonds for PCr, and open squares for ATP. The resulting relative errors as calculated with Eqs. [14] and [20] are shown for $T_R = 1$ s in (E) and $T_R = 2$ s in (F) as solid lines, labeled for each metabolite.

Fishbein set 5 or 10% limits on the allowable difference between observed T_1 's and the intrinsic T_1 's (Tables 3 and 4 of Ref. 5) and show that this is achievable only with SNR efficiencies that are often an order of magnitude lower than the

optimum SNR of the Ernst angle experiment (5). These criteria are not essential for the purpose of quantifying a fully relaxed magnetization and, moreover, may result in significantly less efficient experiments than even the fully relaxed one.

If less efficient experiments are being considered, the fully relaxed experiment is arguably the preferred strategy because it entirely avoids partial saturation and thus also errors in saturation correction due to chemical exchange effects. Although the SNR per unit time in an experiment with 90° flip-angles and a $T_R = 5 T_1$ is still 63% of that of the optimum experiment with 90° pulses and $T_R = 1.256 T_1$, the total measurement time would have to be increased 2.5-fold to realize the same SNR. This may be unacceptable for many human or *in vivo* studies. In contrast, our data indicate that experiments performed with near-optimum T_R 's and flip-angles can be corrected for partial saturation with a single-exponential model in the presence of exchange without introducing significant errors.

Measurements of T_1 are typically derived or should derive from a three-parameter fit to Eq. [15] or the like (10). Our two-site analysis shows that inaccuracies introduced by ignoring multiple-exponential relaxation behavior are reasonably well compensated with the fitting parameters, especially if the T_R values are distributed around the value for which the saturation correction is intended. The progressive saturation experiments that we analyzed were optimized for SNR efficiency by centering the points about the optimum T_R . However, accurately fitting progressive saturation data to an exponential relaxation curve requires the measurement of at least one data point at or near fully relaxed conditions. Therefore, in practice, the progressive saturation T_1 measurement may again be too lengthy to add to the experimental protocol for human studies, necessitating either a separate series of T_1 experiments or the adoption of a more efficient T_1 method such as the dual-angle method (8).

Our analysis shows that the measurement of observed T_1 's using the dual-angle method (8) can predict saturation factors in the presence of chemical exchange with 95% accuracy over an enormous range of exchange rates, with the advantage of SNR performance approaching that achieved at the Ernst angle for the exchanging species. The analysis of the second exponential term in Eqs. [2] and [3] for two-site exchange indicates that the errors due to neglecting exchange are smallest when the least saturated conditions are employed, while nevertheless retaining reasonable SNR (Fig. 1). Comparison of Figs. 4A and 4B with Figs. 4C and 4D shows that the errors introduced by chemical exchange are indeed reduced with increased T_R .

Similar conclusions as for the two-site analysis can be drawn for chemical exchange involving three and four sites. The observed T_1 's in these more complex models may be quite different from the intrinsic T_1 's, as can be seen by comparing values in Fig. 6 with those in Table 2. Nevertheless, the predicted saturation factors and equilibrium magnetization can be accurate to within 95% or better as long as the T_R and flip-angles are chosen for near optimal SNR efficiency. Specifically, as Fig. 5 clearly shows for the three- and four-site exchange models, the errors due to ignoring the effects of chemical exchange and assuming monoexponential relaxation

are minimized by using lower flip-angles and T_R values that are not too short compared to T_1 and which are conducive to high SNR efficiency, in contrast to conclusions (i), (ii), and (iv) in the abstract of Ref. (5).

Although the analysis presented in this paper focused on T_1 values encountered in skeletal and heart muscle in field strengths of around 1.5–2 T, the analysis can readily be scaled to accommodate shorter or longer T_1 's encountered at different field strengths. The SNR efficiency depends only on T_R/T_1 and flip-angle, so it is prudent to scale T_R to compensate for field-dependent T_1 changes. The curves presented herein will be valid for the same *relative* values of T_R , T_1 , and k . The trend showing lower errors at higher values of T_R/T_1 is independent of field strength and, within the constraints of SNR efficiency, the lowest errors from using the single-exponential assumption to correcting saturation will result when longer T_R 's are chosen.

It is recognized that saturation-correction factors derived by methods that neglect chemical exchange are a function of the M_0 's of all of the exchanging species and the exchange rate constants via Eqs. [2], [3], and [14]. This means that, strictly speaking, continuously repeated T_1 measurements would be required in studies where significant changes in one or more of these factors are anticipated. Our analysis suggests that the dual-angle method of measuring T_1 (8) could be used to achieve this with only a small loss of SNR efficiency. It also suggests that the requirement for continuous T_1 measurements could be replaced by just two measurements of T_1 , one performed at the start and one at the end of a study involving monotonic changes in M_0 .

Moreover, the simulation of muscle CK metabolite depletion presented in this paper demonstrates that, for acquisitions under conditions that optimize SNR and reasonable values of the *in vivo* parameters, enormous relative changes in metabolite concentrations have a minor or negligible effect on the saturation-corrected magnetization (Fig. 6). Despite the manifold relative changes in Pi and PCr concentrations associated with the depletion of up to 95% of the PCr and the resulting large changes in reverse k values via Eqs. [21] and [22], the errors in saturation corrections are ≤ 8 or $\leq 4\%$, depending on T_R . Furthermore, these findings are in agreement with the analysis of Binzoni and Cerretelli for a muscle ^{31}P MRS experiment where k values were randomly varied over a large range with little effect on the observed metabolite magnetizations (6). When these authors used, in essence, saturation corrections based only on an initial T_1 experiment, an error of underestimation of up to 12% of the total phosphate resulted as the PCr depletion experiment proceeded. Our data show that this error could be much reduced if the saturation corrections are based on interpolation of relaxation measurements performed at the start and at the end of the depletion experiment.

In summary, the single-exponential model appears to provide a reasonable fit to the observed longitudinal relaxation in

the presence of chemical exchange under experimental conditions that optimize SNR, as they are routinely practiced in skeletal and heart muscle. Indeed, other experimental errors, for example, caused by inaccuracies in the observation pulse flip-angle, low SNR, and biological heterogeneity, are often of larger magnitude (10). Reasonable accuracy is even possible in dynamic experiments in which the equilibrium magnetizations of the exchanging species vary, if measurements are interlaced with dual-angle T_1 measurements.

REFERENCES

1. R. R. Ernst and W. A. Anderson, Application of Fourier transform spectroscopy to magnetic resonance. *Rev. Sci. Instrum.* **37**, 93–102 (1966).
2. P. A. Bottomley, C. J. Hardy, and R. G. Weiss, Correcting human heart ^{31}P NMR spectra for partial saturation. Evidence that saturation factors for PCr/ATP are homogeneous in normal and disease states. *J. Magn. Reson.* **95**, 341–355 (1991).
3. R. G. S. Spencer, J. A. Ferretti, and G. H. Weiss, NMR saturation factors in the presence of chemical exchange. *J. Magn. Reson.* **84**, 223–235 (1989).
4. A. Horská and R. G. Spencer, Measurement of spin-lattice relaxation times and kinetic rate constants in rat muscle using progressive partial saturation and steady-state saturation transfer. *J. Magn. Reson.* **84**, 223–235 (1989).
5. R. G. Spencer and K. W. Fishbein, Measurement of spin-lattice relaxation times and concentrations in systems with chemical exchange using the one-pulse sequence: Breakdown of the Ernst model for partial saturation in NMR spectroscopy. *J. Magn. Reson.* **142**, 120–135 (2000).
6. T. Binzoni and P. Cerretelli, Muscle ^{31}P -NMR in humans: Estimate of bias and qualitative assessment of ATPase activity. *J. Appl. Physiol.* **71**, 1700–1704 (1991).
7. P. A. Bottomley and R. Ouwerkerk, Optimum flip-angles for exciting NMR with uncertain T_1 values. *Magn. Reson. Med.* **32**, 137–141 (1994).
8. P. A. Bottomley and R. Ouwerkerk, The dual-angle method for fast, sensitive T_1 measurement *in vivo* with low-angle adiabatic pulses. *J. Magn. Reson. B* **104**, 159–167 (1994).
9. H. M. McConnell, Reaction rates by nuclear magnetic resonance. *J. Chem. Phys.* **28**, 430–431 (1958).
10. J. L. Evelhoch and J. J. H. Ackerman, NMR T_1 measurements in inhomogeneous B_1 with surface coils. *J. Magn. Reson.* **53**, 52–64 (1983).
11. R. Ouwerkerk, R. F. Lee, R. G. Weiss, and P. A. Bottomley, A new FAST method for *in vivo* measurement of chemical exchange rates. Abstracts of the International Society of Magnetic Resonance in Medicine, 8th Annual Meeting, Denver, p. 421 (2000).
12. R. Ouwerkerk, H. J. Lamb, and C. J. A. van Echteld, More efficient and accurate methods for measuring human cardiac PCr/ATP ratios: Benefits of chemical exchange. Abstracts of the International Society of Magnetic Resonance in Medicine, 6th Annual Meeting, Sydney, p. 1814 (1998).
13. P. A. Bottomley, Non-invasive study of high-energy phosphate metabolism in the human heart by depth resolved ^{31}P NMR spectroscopy. *Science* **229**, 769–772 (1985).